J Mol Model (2009) 15:859–869
DOI 10.1007/s00894-008-0428-3

ORIGINAL PAPER

De(side chain) model of epothilone: bioconformer interconversions DFT study

Danuta Rusinska-Roszak · Marek Lozynski

Received: 8 September 2008 / Accepted: 17 November 2008 / Published online: 20 January 2009

Abstract Using *ab initio* methods, we have studied conformations of the de(sidechain)de(dioxy)difluoroepothilone model to quantify the effect of stability change between the *exo* and *endo* conformers of the epoxy ring. The DFT minimization of the macrolactone ring reveals four low energy conformers, although MP2 predicted five stable structures. The model tested with DFT hybride functional (B3LYP/6–31+G(d,p)) exhibits the global minimum for one of the *exo* forms (**C**), experimentally observed in the solid state, but unexpectedly with the MP2 electron correlation method for the virtual *endo* form (**W**). Using the QST3 technique, several pathways were found for the conversion of the low energy conformers to the other low energy *exo* representatives, as well as within the *endo* analog subset. The potential energy relationships obtained for several *exo* forms suggest a high conformational mobility between three, experimentally observed, conformers. The high rotational barrier, however, excludes direct equilibrium with experimental EC-derived *endo* form **S.** The highest calculated transition state for the conversion of the most stable *exo* **M** interligand to the *endo* **S** form is approximately a 28 kcal/mol above the energy of the former. The two-step interconversion of the *exo* **H** conformer to the *endo* **S** requires at least 28 kcal/mol. Surprisingly, we found that the transition state energy of the **H** form to the virtual *endo* **W** has the acceptable value of about 9 kcal/mol and the next energy barrier for free interconversion of *endo* **W** to *endo* **S** is 13 kcal/mol.

Keywords Anti-cancer · B3LYP · Exo-endo · Intermediates · Transition state

Electronic supplementary material The online version of this article (doi:10.1007/s00894-008-0428-3) contains supplementary material, which is available to authorized users.

D. Rusinska-Roszak · M. Lozynski (✉)
Institute of Chemical Technology and Engineering, Poznan University of Technology,
Pl. M. Sklodowskiej-Curie 2,
60–965 Poznan, Poland
e-mail: Marek.Lozynski@put.poznan.pl

Introduction

As dynamic components of cells, microtubules are crucial in cell reproduction and division processes. In recent years, they have become a natural target for diverse groups of anticancer drugs, any of which derive from natural products [1]. Research has shown that cancer cell apoptosis is caused by the arrest of the cell cycle at the G2/M transition, and it is directly related to an inappropriate formation of the mitotic spindle [2, 3]. We now have a much clearer understanding of the molecular basis of anti-tumor activity of mitosis inhibitors such as taxanes, by elucidating the molecular nature of structural changes that occur in both β- and α-tubulin once stabilized by paclitaxel (Taxol). The determination of the cleft consisting of hydrophobic residues of H1, H7 helix, B7 strand, H6-H7, B9-B10 and M loops, in particular, greatly broadened our knowledge on the mechanism of conformational activation of β-tubulin [4–6] (see also [7]).

The identification of epothilones [8–10] (and other non-taxoid antimitotic compounds), as paclitaxel-like activity drugs [11] has expanded a novel strategy against cancer established on the mitotic arrest of the cell cycle. Of particular interest is the synthetic availability of epothilones from several total syntheses [12, 13] and the bioavailability by myxobacterium culture giving rise to a wide variety of epothilone A **1** (Scheme 1) and related structures [14]. Fermentation followed by one pot partial synthesis with **1**

Scheme 1 Epothilone A **1**, de(side chain)de(dioxy)difluoroepothilone **2** and (*3S,4R*)-3,4-epoxypentan-1-ol acetate **3**

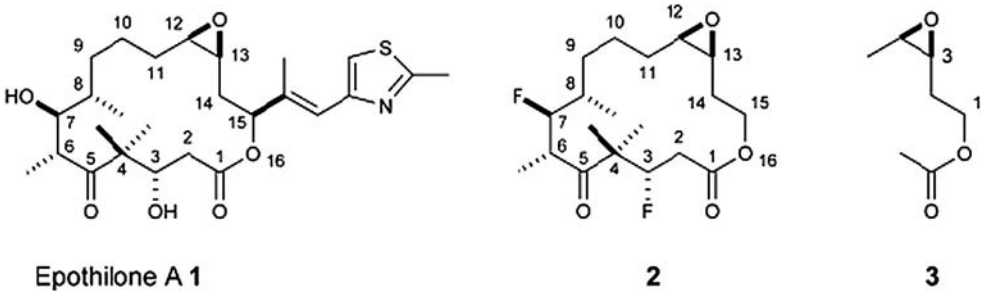

(or its analogs) holds great promise as a future source of semisynthetic drugs [14].

Currently there are at least five epothilones under clinical development: two from Bristol-Myers-Squibb (epothilone B lactam analogue, BMS-247550 and C21 amino epothilone B, BMS-310705), two from Novartis (unmodified epothilone B, EPO906 and C20desmethylsulfanyl epothilone B, ABJ879) and one from Kosan/Sloan-Kettering/Roche (epothilone D, KOS-852) [15, 16]. The first two BMS compounds are the most advanced, and while BMS-247550 is less active [17], it is metabolically more stable than epothilone B, making it a likely candidate for future chemotherapy [18, 19]. Using electron crystallography to study the binding site of epothilone A on α,β-tubulin dimer revealed unexpected differences in the position of the bound ligand [20] toward existing pharmacophore -tubulin models [21–27]. A comparison with paclitaxel epothilone A **1** highlights the expansive and promiscuous binding pocket of β-tubulin in "a unique and qualitatively independent manner" [20]. Its molecule is shifted to the M loop and the tubulin hydrophobic pocket is unoccupied. Data published by Nettles and Snyder [20] clarifies that binding sites and binding forces of taxanes and epothilones on tubulin are distinct. Their findings show that the concept of a common pharmacophore, at least in this case, cannot be considered.

Still at issue is the deciphering of the mechanism(s) in which structurally quite dissimilar drugs, which occupy barely covering binding sites, alter the conformation of β-tubulin, tubulin dimer and, consequently, the stability of microtubule.

It is widely accepted that epothilones form two subsets of conformers in which the epoxide bridge is arranged outward the macrolactone ring, forming a more stable *exo* form [10] or inward, to constitute an *endo* conformer [20]. The presence of two such conformational arrangements increases the number of mutual orientations of carbonyl and hydroxyl groups, leading to several patterns of intramolecular hydrogen bonds and, ultimately, intermolecular hydrogen bonds in contact with a polar protein environment.

Extensive experimental studies ranging from X-ray crystallography [10], electron crystallography [20] and liquid NMR spectroscopy [10, 28–31] contribute to our understanding of the molecular basis of epothilone interactions. In contrast to paclitaxel [4, 5], epothilone ignores the hydrophobic cleft consisting of nine amino acids of the intermediate β-tubulin domain, even without exception of the thiazole ring, which is anchored by His^{227} of H7 helix. The approximately parallel orientation of four carbon-oxygen bonds at the C1-C7 region of epothilone is ideally aligned to easily relocated M-loop residues to engage in the network of hydrogen bonds [20]. Despite the potential of these approaches, further accumulation of data is essential to fully understand the molecular architecture of the ligand-protein complex.

We believe that current research on carcinogenesis and mitotic arrest at the molecular level will facilitate more efficient and specific treatments against different types of cancer. Conformational analysis of highly active anticancer molecules may also enhance our understanding of their individual properties and behavior, their interactions with protein, and their differences in anticancer efficacy. Information collected from organic synthesis and biosynthesis hold promise of yielding a plethora of desired molecular structure subgroups [12, 13] and making both oncology targeted therapy and tailored therapy feasible. Our (and other) computational results may contribute to the key determinants of energy-structure relationships of the epothilone system, as a small, highly active, protein partner, thus suggesting improvement of its future structure.

Methodology

During the past years, only one high level computational approach has been applied to study the role of structural factors involved in the stability of the epothilone system [32]. The overall structure of the epothilone A molecule **1** comprises two conformational almost independent fragments: the 16-membered macrolide ring and the rigid thiazole system, which as a part of the side chain, is linked by two rotatable single bonds. Most likely the relative rotational position of the side chain only partly controls the conformational behavior of the macrolide scaffold and

actually has no profound influence on its conformational profile [28]. So far, however, there have been no high level systematic computational results that account for the side chain - macrolide ring dependence in terms of both structure and energy, probably due to the dimensions of the whole system. Thus, it is first necessary to determine the most appropriate structural model for epothilone to study interconversion pathways of the macrolide system. The influencing lone pairs of the pseudo tetrahedral oxygen atom of epoxide hold particular interest. They are considered to be above and below three-membered ring plane and may primarily interact in TS, or in the *endo* form with both ester oxygens. The oxygen substituents at the 3 and 7 positions (hydroxyl groups), as well as carbonyl positioned at the 5 position of carbon ring, are probably too distant to have a remarkable, transannular effect on the *exo-endo* equilibrium of the system. The fact that the 3,7-dihydroxy-5-oxomacrolactone ring may form several patterns of intramolecular hydrogen bonds presents another challenge. The hydrogen bonding influencing conformer stability may yield the hydrogen bonding dependent energy gap. To address these issues, we created a non-hydroxyl, simplified version that may exploit the unique structural complexity offered by the natural epothilone system and mimic its conformational behavior. The design of a suitable hydroxyl mimetic depends upon the finding of a proper replacement: fluorine is a logical choice given that fluorine is of a similar size [33], electronegativity [34, 35] and ionization potential [36, 37] as the oxygen atom. The issue of the obscuration of conformational energies, in a variety of intramolecular hydrogen bonding interactions, different even with medium torsional angle changes of the macrocycle, is then omitted. To make the epothilone system tractable at a high computational level, we selected de(side chain) structure of original epothilone A.

We substituted the [(*1E*)-1-methyl-2-(2-methyl-4-thiazolyl)ethenyl] side chain with hydrogen. The results reduced, but in the macrolide part, isosteric with epothilone scaffold molecule **2** was employed as the object of the first approach explorative conformational examination and analysis.

All energies and structures reported here were calculated using Gaussian 03 software [38], at the B3LYP/6–31+G(d,p) and MP2/6–31+G(d,p)//B3LYP/6–31+G(d,p) level of theory [39, 40]. We applied the default loose convergence criteria of the Gaussian program. The structures selected were not the result of a complete conformational search. Initial hypotheses for the generation of the representative *exo* and *endo* forms were chosen rather because their molecular geometries were established experimentally by X-ray crystallography (**H** [10]), electron crystallography (**S** [20]), NMR spectroscopy (**M** [29], **T** [28]) or on the basis of QSAR studies (**W** [41], **B** [42]).

To expand the breadth of our conformational studies, we also looked at epothilone family compounds bearing different types of substituents. We used Cambridge Structural Database (CSD) [43] version 5.27 (updated November 2005) searches to locate epothilones containing all structural features, including stereochemical of epothilone A. We explored CDS (Conquest program associated with the base) and found nine structures of a 16-membered macrolide; out of these only four have no ring double carbon-carbon bonds. One structure (VADKER [43]) was epothilone itself (ether solvate), and three other structures have different, atypical to epothilone A or B substituents. These structures were removed and/or reconstructed to give virtual epothilone A structures. Finally, epothilone A was considered in 11 conformations. QAFFEI [43] contains an N-oxide function on the thiazole ring, but after DFT optimization of the epothilone construct was transformed into structure f**M**. Likely MUQLIT [43] *(3R)*-cyano derivative and VADKER [43] gave f**H** geometry found in epothilone A or B crystal structures. WUMKEU [43] (14*S*)-methyl derivative of epothilone B saved its original conformation and is named as conformer f**C**. Moreover, coordinates of the *endo* form of epothilone A bound to tubulin (1TVK [20], after optimization f**S**) or cytochrome P450epoK (1Q5D) [44] were extracted from Protein Data Bank (PDB) files. The optimized 1Q5D rested as the f**T** conformer.

The molecule was converted from one local minimum into another by averaging their structure atom positions with the linear synchronous transit (QST2) [45] standard method, although a manual local intervention was necessary in some cases to obtain realistic geometries for several transition state structures. It became clear that because of the size of the macrolactone ring and probable alternative transition states, the QST2 technique could not exhaust all the possible starting point geometries. It is important to note that other templates were not imposed during the optimization involving the QST3 transition state. In a few cases templates were intended to reproduce the structures of transition states in which the "identity" (at least at LOOSE convergence level) was explicitly stated. Indeed, in four cases the "identity" (energetic and structural) of TSs did not change and was confirmed by QST3. In some cases, the subsequent search for transition states with the quadric synchronous transit approach (QST3) [46] resulted in new intermediate structures.

Transition state and intermediates were initially found using the B3LYP/3–21G level of theory. The structures then were refined using 6–31G, and finally 6–31+G(d,p) basis set. This procedure was applied to find the energy minimized structures more efficiently. Frequency calculations were performed for each minimum and transition state structure to confirm its status by the presence of none or a single imaginary frequency, respectively.

Results

The computational technique was used to investigate conformation energies of a group of epothilone conformers using its de[(1*E*)-1-methyl-2-(2-methyl-4-thiazolyl)ethenyl] de(3,7-dioxy)-3,7-difluoro model **2** (Scheme 1). As the first step of conformational analysis, we carried out the *ab initio* DFT and MP2 energy study (B3LYP/6–31+G(d,p) and MP2/6–31+G(d,p)//B3LYP/6–31+G(d,p) on all stable conformers (or conformers adapted on the basis of its derivatives) reported in the literature (see Methodology). In general, the seven conformations under consideration include two related to Höfle's, precisely established, X-ray structures (**H**) [10], Taylor and Chen's demethylated in the C(14) position structure (**C**) [47], Taylor's proton NMR conformer (**T**) [28], also Carlomagno and Meiler's proton NMR conformer (**M**) [29], krio EC Nettles and Snyder's (**S**) [20]. We also considered Botta's (**B**) [42] and Wang and Snyder's (**W**) [41] virtual structures. For the reasons given above and below, the **H** structure is treated as the reference in assigning the main conformational trends of the model system. The relative energies found in our *ab initio* calculations (B3LYP, ZPVE B3LYP and MP2) on macrolactone are summarized in Table 1. The optimized conformer total and relative energies are given in Table S2.

The geometry of each conformer's macroring is characterized by 16 intraangular torsional angles as presented in Table S3 (see Table S4 for torsional angle values of polar substituents between preceding and following ring atoms). To give insight into the intensity interactions within the macroring, we calculated the root mean square errors (RMS) of 16 macrolide ring atoms of starting epothilone geometries and DFT optimized structures. The errors never meaningfully exceeded 0.5 Å (Table S5) and were considerably low (0.103 Å) for the crystal **H** conformer. Thus our model appears to offer the specific 3D architecture of epothilone polar groups for the conformational stability of the system. The entire set of dihedral angles depicting local dipole-dipole interactions of ring neighboring polar substituents can be found in Table S6, and *syn*-pentane and transannular effects data of the macrolide ring system are given in Tables S7 and S8 respectively.

According to the reported QST3 "common" transition states, for three or four minimum structures, these TSs should have two or three negative eigenvalues. As this is not the case (Figs. 1, 2 and Table S2) we hypothesize that reaction energy path must be much more complex than previously thought, and that locally, the potential energy surface may be very flat. Therefore, the "common" transition state must be considered as the transition state region with a high sensitivity to the computational level. At the calculation level B3LYP/6–31+G(d,p), and lowered precision of convergence, the QST3 procedure determines the most prominent maximum ignoring subtle energy profiles on plateau-like transition multi-state area. Although suitable, but the time demanding MP2 level calculations are out of range of the computational feasibility for the system investigated here.

For each of the three DFT low energy conformers, f**C**, f**M** and f**H,** the oxirane ring has the *exo* orientation toward the macrocycle. Unexpectedly, a rather unstable DFT virtual f**W** *endo* conformer yielded the lowest energy at MP2 and emerged as the fourth possible structure candidate in the set of our difluoroepothilone model conformers. The range of Møller-Plesset correlation energy for stable *exo* DFT conformers does not exceed of 1 kcal/mol, with the smallest correction for f**C** conformer. Interestingly, al-

Table 1 DFT (B3LYP), corrected (ZPVE), correlated energy correction (MP2) relative [a] energies for stable conformations, intermediates and transition states of 15-de(side chain)-3,7-de(dioxy)-3,7-difluoroepothilone at the B3LYP/6-31+G(d,p) and MP2/6-31G+(d,p)//B3LYP/6-31G+(d,p) levels of theory

Symbol	B3LYP	ZPVE	MP2//B3LYP
Conformers			
f**C**	0.03	0	1.34
f**M**	0	0.06	0.67
f**H**	0.86	0.93	1.35
f**T**	4.77	4.95	5.54
f**B**	10.63	10.93	10.89
f**S**	7.23	7.74	6.15
f**W**	3.00	3.32	0
Intermediates			
f**HIT**	5.61	5.75	6.58
f**HIS**	5.50	5.71	6.40
f**MIS1**	3.10	3.16	3.61
f**MIS2**	7.06	7.50	5.30
f**TIC**	0.72	0.69	1.27
Transition states			
$_{fTIC}TS^{fC}$	2.00	1.79	2.78
$_{fM}TS^{fMIS1}$	3.68	3.66	4.21
$_{fC,\ fM,\ fH}ts^{cmmn}$ [b]	4.77	4.99	6.65
$_{fC,\ fM,\ fH,\ fW}ts^{cmmn}$ [c]	6.88	6.38	8.42
$_{fC,\ fM,\ fH,\ fHIT}TS^{cmmn}$ [d]	6.90	7.03	8.30
$_{fH}TS^{fW}$	9.12	9.53	6.56
$_{fH}TS^{fT}$	9.53	9.45	10.81
$_{fH}TS^{fHIS}$	9.89	9.83	10.32
$_{fMIS2}TS^{fS}$	11.57	11.81	11.63
$_{fW}ts^{fS}$	13.15	13.77	11.23
$_{fM,\ fT,\ fTIC}TS^{cmmn}$ [e]	16.08	16.81	16.04
$_{fW}TS^{fS}$	19.19	19.59	16.73
$_{fMIS1}TS^{fMIS2}$	28.07	28.47	24.96
$_{fHIT}TS^{fS}$	28.64	29.07	25.81

[a] kcal*mol^{-1} ; [b] $_{fC,\ fM,\ fH}ts^{cmmn} \approx {}_{fM}ts^{fC} \approx {}_{fH}ts^{fC} \approx {}_{fH}ts^{fM}$;
[c] $_{fC,\ fM,\ fH,\ fW}ts^{cmmn} \approx {}_{fH}ts^{fW} \approx {}_{fH}ts^{fM} \approx {}_{fH}ts^{fC} \approx {}_{fC}ts^{fM} \approx {}_{fC}ts^{fW} \approx {}_{fM}ts^{fW}$;
[d] $_{fC,\ fM,\ fH,\ fHIT}TS^{cmmn} \approx {}_{H}TS^{fHIT} \approx {}_{fH}TS^{fM} \approx {}_{fH}TS^{fC} \approx {}_{fC}TS^{fM} \approx {}_{fC}TS^{fHIT} \approx {}_{fM}TS^{fHIT}$;
[e] $_{fM,\ fT,\ fTIC}TS^{cmmn} \approx {}_{fM}TS^{fT} \approx {}_{fT}TS^{fTIC} \approx {}_{fM,\ fT,\ fTIC}TS^{cmmn}$.

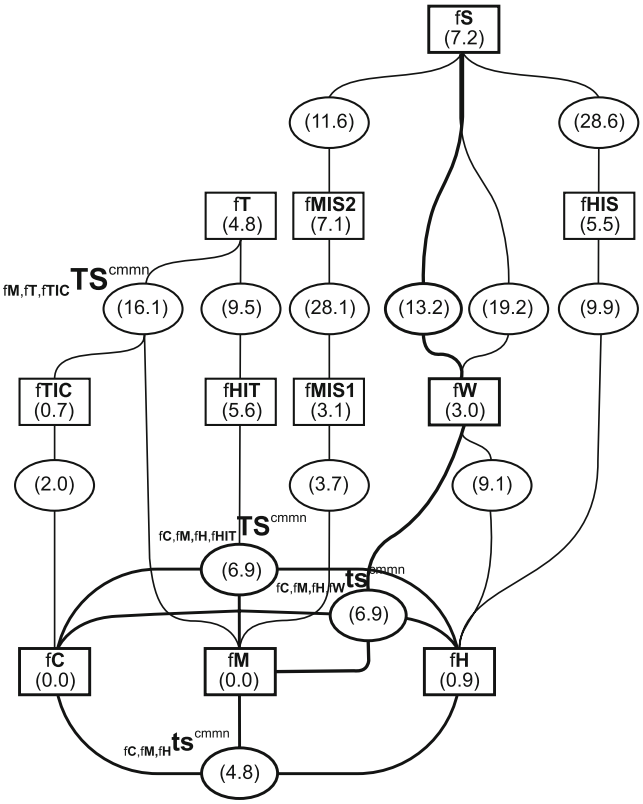

Fig. 1 The map of energy-minimized 15-de(side chain)-3,7-dedioxy-3,7-difluoroepothilone conformers (in rectangles) and transition states (in ovals) with their relative energies (kcal/mol, DFT B3LYP/6–31+G (d,p) basis set) along the alternative paths between rotational states. The heavy line follows the easiest possible path from the most stable conformers f**C**, f**M** and f**H** to the fluorine model of epothilone A f**S** bound to β-tubulin

though the interconversion processes proceed without breaking and forming bonds, the correlation energy for *endo* rotamers is of 2.39 kcal/mol and 4.31 kcal/mol for f**S** and f**W** respectively. The inversion observed between MP2 and DFT energies is probably related to van der Waals interactions; these typically are poorly reproduced by DFT due to the inaccurate treatment of molecular strains, weak repulsions and dispersions.

In contrast, the also virtual, but *exo* f**B** conformer has the highest energy, considerably exceeding 10 kcal/mol global minimum for two computational methods applied. We think this likely due to its peculiar *s-cis* macrolactone conformation. In the *exo* low energy subset, the methylene sequence of ring bonds from C(8) to C(11) is conservatively *ap*, but for the only *endo* stable conformer f**W,** this *ap* orientation is limited to two bonds. Again, the sequence of C(15)-C(3) is the next conformationally established region for all the four difluoroepothilone low energy minima.

Transannular interactions of epoxide and ester groups

Our research focused on the 12,13-epoxide ring, as a structural fragment capable of controlling both interconversion and bioactivity of macrocyclic conformers [cf. 48]. It appears that two symmetric electron lone pairs on the epoxide oxygen atom, acting first with ester and less intensively with polar substituents at 3-, 5-, 7- positions of macrocycle, play a key role in determining the energy relationships of both stable structures and transition states during *exo-endo* conformers transformations and generally define the overall PES of the system. Indeed, the oxirane ring model predicts that an interaction between two lone

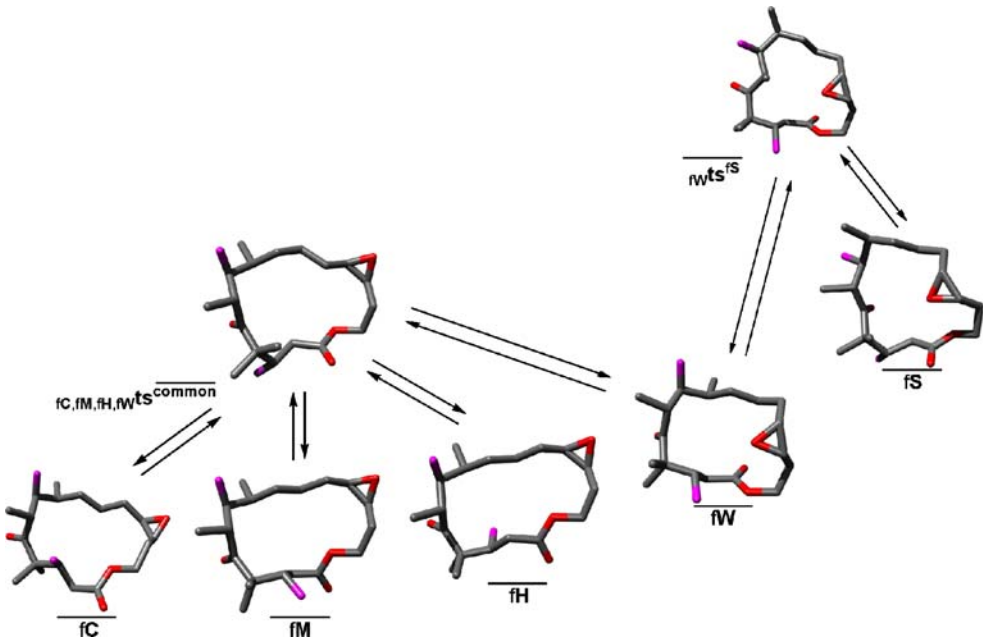

Fig. 2 Structures of stable conformers and transition states along the conformer interconversion pathway, denoted by the heavy line, in Fig. 1 (The image designated $_{fC,\ fM,\ fH,\ fW}ts^{common}$ represents four transition states, structurally closely related, but not identical. Structure of "common", low energy transition state $_{fC,\ fM,\ fH}ts^{common}$ is omitted). Note that the position of a structure in the Figure is only loosely related to its internal energy (thin line below the each guess). Shapes of conformer f**B** and f**T** were omitted because of its marginal importance for *exo-endo* interconversion process due to their relative high energies

pairs of an oxygen atom might occur with any adjacent π system, especially when its plane is perpendicular to the plane of π system [49, cf. 50–52]. Thus the conformational analysis of *endo* conformers of our difluoro model of epothilone can not simply parallel that of the *exo* set. This was made more complex by the need to determine two of their geometric aspects, *i.e.*, the mutual position of the ester group, and distances of its oxygen atoms with respect to the epoxide ring. Therefore, it is reasonable to make the conformational analysis simply in terms of the orientation of the oxirane ring system as *exo* and *endo* toward the macrocyclic ring and in relation to the ester group plane. In conformers that correspond to the *exo* arrangement, the torsional angle of epoxide oxygen and preceding and following macrocycle atoms (O(12)-C(12)-C(11)-C(10) and O(12)-C(13)-C(14)-C(15) respectively), are, without exception, *ap* and give values of these angles of 179° to 187° and of 163° to 182°. For *endo* forms these dihedrals are 47° and −63°, (*i.e.*, both ±*sc*) for f**S**, but 4° and −75° for f**W** (*i.e., sp* and *-sc*), respectively, suggesting the valuable difference also in the part bearing usually the thiazole side chain, but not respected to the model. We would expect the **S** conformer to exhibit another difference: the epoxide oxygen and non-carbonyl oxygen atom of the lactone group have the relative small atomic distance (2.79 Å in original **S**, but 2.99 Å in the DFT f**S** optimized structure, *i.e.*, of 0.05 Å below the sum of van der Waals radii for two oxygen atoms), suggesting the presence of a transannular repulsive interaction. This stereoelectronic feature, probably due to the overlapping of free electron pairs, is a source of the considerable energy difference between energies of **S** and **W** conformers. Our calculations, however, determined a significant difference between two *endo* forms f**W** and f**S**: about 4.2 kcal/mol at B3LYP, but 6.2 kcal/mol at the MP2 level. At room temperature, the only (if present) detectable *endo* conformer may have **W** structure, but it is not clear whether it can rapidly interconvert into **S**.

In optimized both: *endo* f**S** and f**W** conformers, the macrolactone ester group, while not disposed perpendicular to the epoxide plane, has a plane-plane angle of 63° and 71° respectively. This value is typical for all *exo-endo* intermediates (data not shown). In contrast, the angle of all *exo* conformers is rather small (close to 30°), but for f**C** (ZPVE global minimum) the planes are near perfectly parallel (plane-plane angle value is 2°). Although this structural aspect is not fully exploited, we checked the optimized rotamers of (3*S*,4*R*)-3,4-epoxypentan-1-ol acetate **3** (Scheme 1), and the open ester submodel of the investigated macrolactone system conserved the mutual disposition of the epoxy and ester groups in relation to their respective parts of the mother macroring. We concluded that energy for the epoxy ester fragment geometry, based upon six subsequent torsional angles of both free and frozen angles along the epoxypentane chain the *exo*-like type of epoxide orientation, was 0.6 (free) or in the range of 0.7 to 1.7 kcal/mol (frozen) *more* stable than extended (*all trans*) submodel conformer, respectively. For the *endo*-like type of orientation, these numbers are *ca* 0.9 and 1.4 to 2.7 kcal/mol of extra stabilization energy at the MP2//B3LYP level (M. Lozynski, unpublished data). These data were confirmed at optimized MP2 and CCSD(T)//MP2 levels clearly proving that stereoelectronic epoxide and ester group interactions are valuable factors, although not sole determinants, of the *exo-endo* equilibrium of epothilone macroring structures.

In the ideal, non-rigid macrolactone conformation, there is the conformational strong preference of the C(15)-O(16)-C(1)-O(1) unit to be *cis* and close planar, thus preserving the resonance energy of the ester group [53]. In Table S6 we introduce a value of C(15)-O(16)-C(1)-O(1) dihedral as a factor of exploring the effect of the ester group in the stability of the entire molecules. Rejecting the f**B** structure because of its high instability, the *exo* structure f**H**, f**M** and f**C** are comparably stable in light of both B3LYP and MP2 energies. Five of the seven reported conformers show these dihedral values to be negative, but two B3LYP unstable conformers (namely f**T** and f**S**) yield dihedral values up to minus nine degrees. In the *endo* f**S** conformation, macroring strain and/or steric repulsions between the epoxide and non-carbonyl oxygen atom of the ester group are able to splay them apart (C(15)-O(16)-C(1)-O(1) angle is −9.3° for f**S**, but importantly for f**W**, it is only 3.9° (Table S6)), so the observed puckering is probably, at least in part, the source of its higher energy. The modeling study with epoxypentanol acetate submodel **3** similarly demonstrates that the ester group in the **S** macrocycle conformation, with an angle of pucker of -9.3° and with a distance of O(1) and O(12) of 2.99 Å, relaxes in the open structure of f**S** acetate to -5.1° with replacing of interacting oxygens to 3.19Å, highly reducing the strain exceeding the tolerable sum of van der Waals radii (3.04 Å). Interestingly, for a fully relaxed acetate f**W** conformation, the displacement of the ester group from the plane changed negligibly (from 3.9° to 4.1°), exhibiting the non-strained, optimal conformation even in the cyclic macroform (M. Lozynski, unpublished data).

With its relative energy, being 5 kcal/mol less stable, than the global minimum, the f**T** conformer, reported as the less populated NMR structure [28], is the considerable exception. This only conformer of the *exo*-type subset is distinguished by the aforementioned non-planarity of C(15)-O(16)-C(1)-O(1) system with the dihedral of −8.7 degrees. During constraint free, optimization, the f**T** conformer of the epoxy pentanol acetate submodel relaxes the strain to achieve a fully relaxed ester with an angle of only −0.5 degree. Interestingly, these relaxed esters are only

1.1 and 1.6 kcal/mol more stable than their respective constrained f**S** and f**T** analogues (MP2//B3LYP results).

Other structural aspects of conformers stability

Selected data gathered for additional conformational aspects of the macroring and its substituents, *e.g.*, dipole - dipole interactions, *syn*-pentane effects, and transannular interactions obtained by DFT methods are reported in Tables S6–S8. These structural data offer no simple explanation to elucidate the (in)stability of individual conformers. However, when analyzed together with ring structural aspects, these data can help identify the macroring and its substituents as playing the most prominent role in the control of conformational processes and/or having a significant impact on the stability of the conformational system.

Epothilone B (*(*12*R-)* methyl homologue of **1**), having **B** conformation was used (as a microtubule stabilizing an antimitotic agent) in 3D QSAR studies [42] as interacting with β-tubulin to develop the combined pharmacofore generation and pseudoreceptor modeling approach. Conformer f**B** has three structural factors that convincingly determine the source of its instability. First, it has *s-cis* conformation, uncommon for esters and macrolactones and due to Schweizer-Dunitz rule [53] highly enhances the total energy of the system (*s-cis* methyl acetate is 8.85 kcal/mol less stable then *s-trans* conformer at B3LYP/6–31+G(d,p) level; M. Lozynski, unpublished results). Secondly, the carbonyl at C(5) is directed inward. In this unique, concave conformation, it strongly interacts with its local environment: torsional angles of f**B** DFT conformer are the cause of strain: dihedral O(5)-C(5)-C(6)-C(7) is -42.0°, but O(5)-C(5)-C(4)-C(3) was found to be eclipsed of 9.9°. The oxygen atom at C(5) transannularly strongly operates against hydrogens at C(6) and C(10): O(5)-H(6) is 2.38 Å and O(5)-H(10) is 2.37 Å, respectively. Curiously, this conformer avoids any hydrogen-hydrogen interactions common in other conformers, as well as the torsional strains of many substituents with the macroring. Instead one *ac* and a single *syn*-pentane tension actually occurs. Thirdly, two overlapping dipole vectors of *exo* epoxide and carbonyl are strengthened by a local interaction of the lactone group and the neighboring fluorine array and form a system that can presumed to be a cause of the substantial dipole moment (6.27D).

The less populated, NMR-fluoroanalogue f**T** conformer has a calculated energy of up to 5 kcal/mol above the global minimum (Table 1). Nonplanarity of the ester group of the f**T** conformer provides only a partial explanation of its relative instability (see above). The source of its high energy may be torsional interactions in the ring as surroundings of both sides of the oxirane bridge are strictly eclipsed. The non preferred *ac* torsional angle of one of the methyl groups at C(4) and torsions of the macrolide ring: both [C(7)-C(8)-C(9)-C(10) and C(8)-C(9)-C(10)-C(11)] are -*sc*. The remaining stable structures have torsional angles more or less antiperiplanar for the first, and perfect *ap* for the second sequence of macrocyclic atoms. Interestingly, the stable f**C** conformer has a synperiplanar folding in the ketone region: for C(3)-C(4)-C(5)-C(6) torsion is −13.4°.

Generally the stable f**H**, f**M** and f**C** avoid the dipole-dipole effect, instead exhibiting a perpendicular or rather anti parallel orientation (Table S6). Conformer f**H**, an *exo* subset member, exhibits one such polar interaction in the range of 40 degrees, and only the f**T** conformer has an additional carbonyl-(carbon-fluorine) bond in an almost parallel direction with dihedral O(5)-C(5)···C(7)-F(7) of −11.8°. Total dipole moment of f**T** of 3.70D is average, probably due to the mutual reduction of the resultants of two carbonyls and the dipole of the epoxide system and as the nature of two dipoles of carbon fluorine bonds. In addition to the regular transannular interactions of hydrogens at C(11) and C(14) independent of the *exo-endo* kind of stereochemistry, f**T** conformer performs H(7)-H(10), distinctly exceeding the 0.2 Å threshold of the sum of van der Waals radii. Finally, two *syn*-pentane effects of C(5)-C(6) with C(8)-C(9) and C(12)-C(13) with C(15)-C(16) bonds supplement a list of its energy increasing factors. Likely, the reference f**H** conformer exhibits four *syn*-pentane effect features, much more than other *exo*-forms, but without jeopardizing its stability.

Here, we should direct our attention to the high stability of the intermediate f**TIC**. This progenitor of f**T** and f**C** *exo*-conformers, but with an RMS error >0.85 Å for the ring atoms, only appears to resemble its experimentally derived precursors. In fact, f**TIC** has almost the same torsional angles as f**T** and f**C** in the environment of the ester group (from C(14) to C(4)). The +*ac* strain, existing in the proximity of ketone carbonyl of f**T**, f**TIC** transfers on the carbonyl opposite side, closer to the ester group. Our calculations based on 3,4-epoxypentan-1-ol acetate submodel **3** prove that the ester and epoxide system is less stable than that of f**T** by 0.7–0.8 kcal/mol (depending on the calculation level) and almost as stable as the acetate analog of conformer f**C** (0.1 kcal/mol of difference). However it is more stable than 1.4 kcal/mol for *all trans* conformation of this model. The intermediate f**TIC** is exceptional because it avoids the torsional strain around the epoxide function having *ap* and *sc* conformations rather than the common ± *ac* arrangement. The low total energy of the whole system is most likely determined by the last structural feature and the almost ideal compensation of local dipole moments (total dipole is 1.74D). Two torsional interactions of C(4)

methyl groups and transannular interactions of O(5) and H (2) do not appear to exert a marked influence on the total energy of this conformer.

We directed special attention to conformer f**S** because it is a derivative of the first, well documented bioconformer [20]. As mentioned above, its high energy cannot be simply explained in terms of *exo-endo* isomerism. On the one hand, the high relative energy (7.2 kcal/mol) of the DFT structure shows the marginal role of the stabilizing effect of the oxirane ester array. The high energy of the f**S** conformer may result not only from several transannular interactions (two of them exceeding the 0.3 Å threshold), but from as many as five ±*ac* torsions of atoms forming a 16-membered ring (three of them are almost exactly (±15° criterion) eclipsed). On the other hand, torsion interactions of ring substituents with the ring itself and *local* coordination of single dipoles do not exist. Thus, we suggest the importance of the additivity of numerous dipoles of the conformer to account for the final energy score.

The analysis of the f**S** structure shows that although carbon-fluorine bonds, surrounding the ketone group, do not form very acute dihedral angles to each other, the energy of the whole molecule effectively grows as a summary effect of carbon-fluorine dipoles (dihedral angle of F(5)-C(5)···C(7)-F(7) is only 21.7°) and is enhanced by the *endo* oriented oxirane dipole. Importantly, the total dipole moment (6.82D) dominates the set of stable conformers of our difluoro model collection.

Intermediate f**HIS** has a typical RMS error of 1.04 Å and 0.88 Å for 16 atoms of the macroring, respectively and does not resemble either f**H** or f**S** structures. In contrast, the intermediate f**MIS1** closely resembles the structure of its precursor f**M** but only between C(9) and C(15) carbon atoms and in some area of both aldol functionalities although the RMS calculated for the atoms of the whole rings is near 0.9 Å. The intermediate f**MIS2** resembles much more closely its progenitor f**S** (RMS=0.519 Å), but with the exception of ring three bonds within aldol functionalities RMS is 0.263 Å for 13 ring atoms. This is not the case with f**HIS** intermediate because similarity in conformational patterns is equally spread to several sections.

Kinetics of exo-endo interconversions

A careful computational analysis of the epothilone macroring system interconversions kinetics may add new depth of the mechanistic understanding of the potent epothilones as promoters of tubulin polymerization. A major problem of these studies is the limited potential of available computational resources to perform calculations at a confident level of theory. Thus the problem may be solved by reduction to a simpler model in order to obtain *ab initio* energies and barrier interconversions values for both conformers and intermediates. In the present study we graphically present a simplified, de(side chain) dedioxy difluoro model **2** and map of energy minimized structures with their relative energies (B3LYP/6–31+G(d,p) level) (Fig. 1).

These studies reveal that the two most stable f**C**, conformers, f**M** and ubiquitous f**H** mutually convert each other at room temperature with small energy barriers of 4.8 or 6.9 kcal/mol. In fact, the latter value corresponds to two degenerated transition states. One of them is "common" for the three, experimentally proven macrolactone scaffolds. Moreover, the transition state is linked to the f**T**, NMR derived epothilone pattern (f**HIT** is the necessary intermediate). More importantly, these findings define the alternative transition state structure that is "common" for *exo* f**C**, f**M** and f**H** and *endo* f**W** conformers. It also shows the possibility of *exo-endo* equilibrium and points out the direction to the transformation to the EC spectroscopy derived *endo* f**S** structure. The relatively stable f**W** conformer seems to be the indispensable intermediate (see thick line on Fig. 1). Figure 2 shows the shortest possible way of the stable structures f**C**, f**M** and f**H** to the f**S** bioconformer. Note that the transition energies from the virtual *endo*, to the experimental *endo* (13.2 kcal/mol for DFT, but 11.2 for MP2) still seem quite high even in comparison with huge $_{\mathbf{fMIS1}}\mathbf{TS}^{\mathbf{fMIS2}}$ or $_{\mathbf{fHIS}}\mathbf{TS}^{\mathbf{fS}}$ barriers.

The goal of this extended search is to find a straightforward, one step *exo-endo* transformation which starts with the f**M**, experimental β-tubulin induced template and includes the f**S**, final product. Although we refer to two other ways from a stable *exo* structure to a bioactive f**S** conformer, a direct, intermediate-free, route was not found. Figure 1 shows that two significant conformational isomers experimentally shaped by the interaction with β-tubulin, (*i.e.*, f**M** and f**S**) need as many as two intermediates, f**MIS1** and f**MIS2,** and consequently three transition states.

The transformation of *exo* into *endo* conformation could occur through similar transition states $_{\mathbf{fMIS1}}\mathbf{TS}^{\mathbf{fMIS2}}$ and $_{\mathbf{fHIS}}\mathbf{TS}^{\mathbf{fS}}$, respectively (Table S9). However the transition state energies estimated above 28 kcal/mol are significantly too high.

Obviously, the conformational changes of the *exo-endo* transformation require the participation of two bonds directly neighboring the oxirane bridge. It appears that each, aforementioned transition state requires two appreciable conformational change. In the case of $_{\mathbf{fMIS1}}\mathbf{TS}^{\mathbf{fMIS2}}$ they are located far away from each other and occur with engagement of C(1)-C(2) and the tandem of C(10)-C(11) and C(11)-C(12) bonds (Table S9). In the case of $_{\mathbf{fHIS}}\mathbf{TS}^{\mathbf{fS}}$ the agitated bonds C(6)-C(7) and C(8)-C(9) lay in the proximity of each other. Thus, the two energy demanding transition states could exist through participation of one

polar, (ester or ketone) functionality and one non polar (methylene) chain part of the model molecules.

Both high energy transition states predicted should exhibit Hammond behavior [54, 55], and are *late* (*i.e.*, product-like) transition states, having their torsional angles at conformational change sites like the higher energy intermediate (f**MIS2**) or product (f**S**), respectively. The *exo-endo* transformation needs, in addition, the agitation of several bonds. In the case of f**MIS1** → $_{\text{fMIS1}}$**TS**$^{\text{fMIS2}}$ → f**MIS2** its transition relies on a simple fluctuation. This means that the torsion angle deviates and again returns approximately to its former value. The f**HIS** → $_{\text{fHIS}}$**TS**$^{\text{fS}}$ → f**S** transition is more complex because some agitated bonds change their torsional angles gradually (*cf.* changes of dihedrals C(16)-C(1)-C(2)-C(3), C(3)-C(4)-C(5)-C(6) and C(10)-C(11)-C(12)-C(13)) (Table S9). This complex mechanism also works for both alternative $_{\text{fH}}$**ts**$^{\text{fW}}$ and $_{\text{fH}}$**TS**$^{\text{fW}}$ low energies transition states, although the deviation changes strongly dominate over gradual changes of agitated bonds (Table S9). A comparison of ring torsional angles for the former (the lowest *exo-endo* energy transition state $_{\text{fH}}$**ts**$^{\text{fW}}$) with f**H**, qualifies it as the *early* transition state. The later one $_{\text{fH}}$**TS**$^{\text{fW}}$ (more rich in energy by about 2 kcal/mol), has the oxirane part of the transition state strictly features of the early transition state, but dihedrals of three bonds (namely, C(16)-C(1)-C(2)-C(3), C(9)-C(10)-C(11)-C(12) and C(14)-C(15)-C(16)-C(1)) suggest the end of transformation in these sites even at this stage. The observed, non homogenized mechanism argues in favor of the *exo-endo* transformation in a non-concerted manner and shows that macroring interconversions may occur locally with different speeds. While some parts of functionalized macroring participate in the *exo-endo* transformation of their flexible structure and quickly attain final conformation, others are appreciably slower. We note the importance of such cooperation among macroring bonds and emphasize the need to account for the synergy in the lowering of the total transition state energy.

These findings indicate the usefulness of molecular modeling studies at the *ab initio* level to investigate, and perhaps predict, conformational control factors, and to some extent, stereoselection in the biological systems.

Conclusions

By considering relative energies of calculated conformers, we conclude that the epothilone model molecule **2** at room temperature exists primarily as a mixture of at least four distinct *exo* conformers, probably in equilibrium with one *endo* conformer. Thus, the previous conformational paradigm, comprising only **H** and **T** (here perhaps **TIC**) types of conformations, is incomplete. **M**, **C** and **W** structures are also accessible (all lay below, or less than 3 kcal/mol above, the **H**). We are aware that solvent effects are also important and might significantly change the relative stabilities of the considered conformers.

The identification of transition states between many low energy structures enabled us to determine the multi step pathways to full intercoversion between the experimentally predicted, low energy *exo,* and both virtual and EC *endo* conformers. Within the limits of this model, we observed that *exo* and *endo* conformers of molecule can easily interconvert with key intermediate *endo* **W** virtual conformer. These data strongly suggest that a rigid, planar epoxide ring, with the usually *anti* (or sometimes *anti* and *gauche*) C(8)-C(11) methylene sector, behaves as an integrated unit and the steric and polar interactions between its oxygen atom and the rest of the non-symmetric environment of the macrocycle, does not energetically control *exo-endo* interconversion. We believe that the **W** conformer has significance for the complete side (*i.e.*, having side chain) chain epothilone equilibrium. The perfect QSAR free energy correlation result for measured and predicted affinity constants of epothilone family holds great promise [41].

Our calculations are in agreement with the recent NAMFIS [57] based results of the Carlomagno [58] group and highlight: the diversity of epothilone A conformers, the presence of NMR epothilone-tubulin complex **M** scaffold in considerable extent, and exclude the discernible participation of EC-*endo* **S** [20] pattern. This important conformational change may be so subtle that the intramolecular hydrogen bonds must additionally influence or control energy elements. The absence of hydroxyl groups in our model excludes the formation of intramolecular hydrogen bonds, which are possible in the full epothilone structure and also might exert an increase of internal energy within the f**T** and/or f**S** conformers. If true, this underestimation of stability argues for a weakness of the assumed equivalence and subsequent substitution of the hydroxyl group on the fluorine atom, and it limits the scope of conclusions drawn strictly from presented conformational analysis. Systematic computational studies addressing this issue, including solvent effects approach by SCRF model, are in progress and will be the subject of the next report of our group.

Acknowledgments This study was supported by Poznan University of Technology /DS 32/045/2007. The authors are grateful to Professor M. Botta (Università degli Studi di Siena, Siena, Italy), Professor R. E. Taylor (University of Notre Dame, Notre Dame, IN), Professor J. P. Snyder and Dr M. Wang (Emory University, Atlanta, GA), Professor J. Meiler (Vanderbilt University, Nashville, TN) for providing original coordinates of conformers to prepare initial guesses for the generation of epothilone representatives. We also acknowledge Poznanskie Centrum Superkomputerowo-Sieciowe, Poland for computational time.

References

1. Altmann K-H, Gertsch J (2007) Anticancer drugs from nature-natural products as a unique source of new microtubule-stabilizing agents. Nat Prod Rep 24:327–357
2. Jordan MA (2002) Mechanism of action of antitumor drugs that interact with microtubules and tubulin. Curr Med Chem Anti-Cancer Agents 2:1–17
3. Jordan MA, Wilson L (2004) Microtubules as a target for anticancer drugs. Nat Rev Cancer 4:253–265
4. Snyder JP, Nettles JH, Cornett B, Downing KH, Nogales E (2001) The binding conformation of Taxol in β-tubulin: a model based on electron crystallographic density. Proc Natl Acad Sci USA 98:5312–5316
5. Löwe J, Li H, Downing KH, Nogales E (2001) Refined structure of α-beta tubulin from zinc-induced sheets stabilized with taxol. J Mol Biol 313:1045–1057
6. Johnson SA, Alcaraz AA, Snyder JP (2005) T-Taxol and the electron crystallographic density in β-tubulin. Org Lett 7:5549–5552
7. Kingston DGI, Bane S, Snyder JP (2005) The taxol pharmacophore and the T-taxol bridging principle. Cell Cycle 4:279–289
8. DE 4138042 1993 (1993) Chem Abstr 120:52841
9. Gerth K, Bedorf N, Höfle G, Irschik H, Reichenbach H (1996) Epothilons A and B: antifungal and cytotoxic compounds from Sorangium cellulosum (Myxobacteria). J Antibiot 49:560–563
10. Höfle G, Bedorf N, Steinmetz H, Schomburg D, Gerth K, Reichenbach H (1996) Epothilone A and B - novel 16-membered macrolides with cytotoxic activity: isolation, crystal structure, and conformation in solution. Angew Chem Int Ed 35:1567–1569
11. Bollag DM, McQueney PA, Zhu J, Hensens O, Koupal L, Liesch J, Goetz M, Lazarides E, Woods CM (1995) Epothilones, a new class of microtubule-stabilizing agents with a taxol-like mechanism of action. Cancer Res 55:2325–2333
12. Nicolaou KC, Roschangar F, Vourloumis D (1998) Chemical biology of epothilones. Angew Chem Int Ed 37:2014–2045
13. Nicolaou KC, Ritzén A, Namoto K (2001) Recent developments in the chemistry, biology and medicine of the epothilones. Chem Commun 1523–1535
14. Altmann K-H (2004) The merger of natural product synthesis and medicinal chemistry: on the chemistry and chemical biology of epothilones. Org Biomol Chem 2:2137–2152
15. Borzilleri RM, Vite GD (2002) Epothilones: new tubulin polymerization agents in preclinical and clinical development. Drugs Fut 27:1149–1163
16. Altmann K-H (2005) Recent developments in the chemical biology of epothilones. Curr Pharm Des 11:1595–1613
17. Borzilleri RM, Zheng X, Schmidt RJ, Johnson JA, Kim S-H, DiMarco JD, Fairchild CR, Gougoutas JZ, Lee FYF, Long BH, Vite GD (2000) A novel application of a Pd(0)-catalyzed nucleophilic substitution reaction to the regio- and stereoselective synthesis of lactam analogues of the epothilone natural products. J Am Chem Soc 122:8890–8897
18. Gianni L (2007) Ixabepilone and the narrow path to developing new cytotoxic drugs. J Clin Oncol 25:3389–3391
19. De Jonge M, Verweij J (2005) The epothilone dilemma. J Clin Oncol 23:9048–9050
20. Nettles JH, Li H, Cornett B, Krahn JM, Snyder JP, Downing KH (2004) The binding mode of epothilone A on α,β-tubulin by electron crystallography. Science 305:866–869
21. Winkler JD, Axelsen PH (1996) A model for the taxol (paclitaxel)/epothilone pharmacophore. Bioorg Med Chem Lett 6:2963–2966
22. Ojima I, Chakravarty S, Inoue T, Lin S, He L, Horwitz SB, Kuduk SD, Danishefsky SJ (1999) A common pharmacophore for cytotoxic natural products that stabilize microtubules. Proc Natl Acad Sci USA 96:4256–4261
23. Giannakakou P, Gussio R, Nogales E, Downing KH, Zaharevitz D, Bollbuck B, Poy G, Sackett D, Nicolaou KC, Fojo T (2000) A common pharmacophore for epothilone and taxanes: molecular basis for drug resistance conferred by tubulin mutations in human cancer cells. Proc Natl Acad Sci USA 97:2904–2909
24. He L, Jagtap PG, Kingston DG I, Shen H-J, Orr GA, Horwitz SB (2000) A common pharmacophore for taxol and the epothilones based on the biological activity of a taxane molecule lacking a C-13 side chain. Biochemistry 39:3972–3978
25. Lee KW, Briggs JM (2001) Comparative molecular field analysis (CoMFA) study of epothilones-tubulin depolymerization inhibitors: pharmacophore development using 3D QSAR methods. J Comput-Aided Mol Design 15:41–55
26. Manetti F, Maccari L, Corelli F, Botta M (2004) 3D QSAR models of interactions between β-tubulin and microtubule stabilizing antimitotic agents (MSAA): a survey on taxanes and epothilones. CurrTop MedChem 4:203–217
27. Day BW (2000) Mutants yield a pharmacophore model for the tubulin-paclitaxel binding site. Trends Pharmacol Sci 21:321–323
28. Taylor RE, Zajicek J (1999) Conformational properties of epothilone. J Org Chem 64:7224–7228
29. Carlomagno T, Blommers MJJ, Meiler J, Jahnke W, Schupp T, Petersen F, Schinzer D, Altmann K-H, Griesinger C (2003) The high-resolution solution structure of epothilone a bound to tubulin: an understanding of the structure-activity relationships for a powerful class of antitumor agents. Angew Chem Int Ed 42:2511–2515
30. Carlomagno T, Sánchez VM, Blommers MJJ, Griesinger C (2003) Derivation of dihedral angles from CH-CH dipolar-dipolar cross-correlated relaxation rates: a C-C torsion involving a quaternary carbon atom in epothilone A bound to tubulin. Angew Chem Int Ed Engl 42:2515–2517
31. Reese M, Sánchez-Pedregal VM, Kubicek K, Meiler J, Blommers MJJ, Griesinger C, Carlomagno T (2007) Structural basis of the activity of the microtubule-stabilizing agent epothilone a studied by NMR spectroscopy in solution. Angew Chem Int Ed 46:1864–1868
32. Ballone P, Marchi M (1999) A density functional study of a new family of anticancer drugs: paclitaxel, taxotere, epothilone, and discodermolide. J Phys Chem A 103:3097–3102
33. Bondi A (1964) van der Waals volumes and radii. J Phys Chem 68:441–451
34. Jolly WL, Perry WB (1973) Estimation of atomic charges by an electronegativity equalization procedure calibrated with core binding energies. J Am Chem Soc 95:5442–5450
35. Jolly WL, Perry WB (1974) Calculation of atomic charges by an electronegativity equalization procedure. Inorg Chem 13:2686–2692
36. Huheey JE, Keiter EA, Keiter RL (1993) Inorganic chemistry: principles of structure and reactivity, 4th edn. Harper Collins, New York
37. James AM, Lord MP (1992) Macmillan's chemical and physical data. Macmillan, London
38. Frisch MJ, Trucks GW, Schlegel HB, Scuseria GE, Robb MA, Cheeseman JR, Montgomery JA, Vreven T, Kudin KN, Burant JC, Millam JM, Iyengar SS, Tomasi J, Barone V, Mennucci B, Cossi M, Scalmani G, Rega N, Petersson GA, Nakatsuji H, Hada M, Ehara M, Toyota K, Fukuda R, Hasegawa J, Ishida M, Nakajima T, Honda Y, Kitao O, Nakai H, Klene M, Li X, Knox JE, Hratchian HP, Cross JB, Adamo C, Jaramillo J, Gomperts R, Stratmann RE, Yazyev O, Austin AJ, Cammi R, Pomelli C, Ochterski JW, Ayala PY, Morokuma K, Voth GA, Salvador P, Dannenberg JJ, Zakrzewski VG, Dapprich S, Daniels AD, Strain MC, Farkas O, Malick DK, Rabuck AD, Raghavachari K,

Foresman JB, Ortiz JV, Cui Q, Baboul AG, Clifford S, Cioslowski J, Stefanov BB, Liu G, Liashenko A, Piskorz P, Komaromi I, Martin RL, Fox DJ, Keith T, Al-Laham MA, Peng CY, Nanayakkara A, Challacombe M, Gill PMW, Johnson B, Chen W, Wong MW, Gonzalez C, Pople JA (2004) Gaussian 03 Revision C02 Gaussian Inc, Wallingford CT

39. Becke AD (1988) Density-functional exchange-energy approximation with correct asymptotic behavior. Phys Rev A 38:3098–3100
40. Møller C, Plesset MS (1934) Note on an approximation treatment for many-electron systems. Phys Rev 46:618–622
41. Wang M, Xia X, Kim Y, Hwang D, Jansen JM, Botta M, Liotta DC, Snyder JP (1999) A unified and quantitative receptor model for the microtubule binding of paclitaxel and epothilone. Org Lett 1:43–46
42. Manetti F, Forli S, Maccari L, Corelli F, Botta M (2003) 3D QSAR studies of the interaction between β-tubulin and microtubule stabilizing antimitotic agents (MSAA). A combined pharmacophore generation and pseudoreceptor modeling approach applied to taxanes and epothilones. Il Farmaco 58:357–361
43. CSD: The Cambridge Structural Database Cambridge Crystallographic Data Centre 12 Union Road Cambridge CB21EZ UK, www.ccdc.cam.ac.uk
44. Nagano S, Li H, Shimizu H, Nishida C, Ogura H, Ortiz de Montellano PR, Poulos TL (2003) Crystal structures of epothilone D-bound, epothilone B-bound, and substrate-free forms of cytochrome P450epoK. J Biol Chem 278:44886–44893
45. Peng C, Schlegel HB (1993) Combining synchronous transit and quasi-Newton methods to find transition states. Isr J Chem 33:449–454
46. Peng C, Ayala PY, Schlegel HB, Frisch MJ (1996) Using redundant internal coordinates to optimize equilibrium geometries and transition states. J Comput Chem 17:49–56
47. Taylor RE, Chen Y, Beatty A, Myles DC, Zhou Y (2003) Conformation-activity relationships in polyketide natural products: a new perspective on the rational design of epothilone analogues. J Am Chem Soc 125:26–27
48. Heinz DW, Schubert W-D, Höfle G (2005) Much anticipated - the bioactive conformation of epothilone and its binding to tubulin. Angew Chem Int Ed 44:1298–1301
49. Abraham RJ, Castellazzi I, Sancassan F, Smith TAD (1999) Conformational analysis, Part 31.[1] A theoretical and lanthanide induced shift (LIS) investigation of the conformations of some epoxides. J Chem Soc Perkin Trans 2:99–106
50. Vila A, Mosquera RA (2003) AIM study on the protonation of methyl oxiranes. Chem Phys Lett 371:540–547
51. Coxon JM, Thorpe AJ, Smith WB (1999) Potential energy surface for the acid- and BF_3-catalyzed rearrangement of methylpropene oxide. J Org Chem 64:9575–9586
52. Carlier PR, Deora N, Crawford TD (2006) Protonated 2-methyl-1,2-epoxypropane: a challenging problem for density functional theory. J Org Chem 71:1592–1597
53. Schweizer WB, Dunitz JD (1982) Structural characteristics of the carboxylic ester group. Helv Chim Acta 65:1547–1554
54. Hammond GS (1955) A correlation of reaction rates. J Am Chem Soc 77:334–338
55. Smith MB, March J (2007) March's advanced organic chemistry: reactions mechanisms and structure, chapter 6, 6th edn. Wiley, New York
56. Eliel EL, Wilen SH (1994) Stereochemistry of organic compounds, chapter 11. Wiley, New York
57. Cicero DO, Barbato G, Bazzo R (1995) NMR analysis of molecular flexibility in solution: a new method for the study of complex distributions of rapidly exchanging conformations. application to a 13-residue peptide with an 8-residue loop. J Am Chem Soc 117:1027–1033
58. Erdelyi M, Pfeiffer B, Hauenstein K, Fohrer J, Gertsch J, Altmann K-H, Carlomagno T (2008) Conformational preferences of natural and C3-Modified epothilones in aqueous solution. J Med Chem 51:1469–1473